CFD ANALYSIS OF THE COMBUSTION PROCESS OF LEATHER RESIDUALS GASIFICATION FUEL GAS: INFLUENCE OF FUEL MOISTURE CONTENT

Antonietti, Anderson José
Univ. Reg. Integrada do Alto Uruguai e das Missões – URI. Av. Sete de Setembro, 1621, CEP 99700-000, Erechim, RS – Brasil.
andernietti@yahoo.com.br

Beskow, Arthur Bortolin
Univ. Reg. Integrada do Alto Uruguai e das Missões – URI. Av. Sete de Setembro, 1621, CEP 99700-000, Erechim, RS – Brasil.
arthur@uricer.edu.br

Indrusiak, Maria Luiza Sperb
Universidade do Vale do Rio dos Sinos – UNISINOS. Av. Unisinos, n. 950, CEP 93022-000, São Leopoldo – RS – Brasil
mlsperb@unisinos.br

da Silva, Cristiano Vitorino
Univ. Reg. Integrada do Alto Uruguai e das Missões – URI. Av. Sete de Setembro, 1621, CEP 99700-000, Erechim, RS – Brasil.
cristiano@uricer.edu.br

Abstract. *This work presents a numerical study of the combustion process of leather residuals gasification gas, aiming the improvement of the process efficiency, considering different concentrations of water on the gas. The heating produced in this combustion process can be used to generation of thermal and/or electrical energy, for use at the leather industrial plant. However, the direct burning of this leather-residual-gas into the chambers is not straightforward. The alternative in development consists in processing this leather residuals by gasification or pyrolysis, separating the volatiles and products of incomplete combustion, for after use as fuel in a boiler. At these processes, different quantities of water can be used, resulting at different levels of moisture content in this fuel gas. This humidity can affect significantly the burning of this fuel, producing unburnt gases, as the carbon monoxide, or toxic gases as NO_x, which must have their production minimized on the process, with the purpose of reducing the emission of pollutants to the atmosphere. Other environment-harmful-gases, remainings of the chemical treatment employed at leather manufacture, as cyanide, and hydrocarbons as toluene, must burn too, and the moisture content has influence on it. At this way, to increase understanding of the influence of moisture in the combustion process, it was made a numerical investigation study of reacting flow in the furnace, evaluating the temperature field, the chemical species concentration fields, flow mechanics and heat transfer at the process. The commercial CFD code CFX © Ansys Inc. was used. Considering different moisture contents in the fuel used on the combustion process, with this study was possible to achieve the most efficient burning operation parameters, with improvement of combustion efficiency, and reduction of environmental harmful gases emissions. It was verified that the different moisture contents in the fuel gas demand different operation conditions and have a significant effect on the pollutant formation.*

Keywords*: Leather, CFD, Combustion, Finite Volumes, Waste to Energy.*

1. INTRODUÇÃO

The development of viable technologies that make profitable the use of non-conventional sources of energy in place of fossil fuels is one of the major technological challenges of today. Global warming due to the emissions generated by fossil fuels combustion, and the finite reserves of that fuels, are among the main reasons for that. In the other hand, the usual disposal of leather residuals in landfills are no longer permitted because of the harmful contamination of underground water and the emission of methane generated by the decomposition of organic raw material. An emergent and great problem is also the difficulty to allocate adequate land areas for waste disposal. Besides, technical and environmental requirements for direct burning of such residuals make that task not so simple.

The process of gasification of leather residuals is similar to the firing by pyrolysis (burning process rich in H_2O and poor in O_2, consisting in the thermal degradation, causing the chemical decomposition by heat), but it occurs at a higher temperature. The main effect of moisture on the combustion is the dilution of the combustible gases produced by the gasification of the solid material. As that process occurs in a extremely moist environment, alteration of moisture of the leather residuals and the residence time of the gases in the gasifier influence the level of moisture of the fuel gas, which may modify the characteristics of the burning process in the reactor and the production of pollutants.

Bahillo et al. (2004) performed experimental studies on fluidized bed combustion of leather scraps. The HCN and NH3 concentrations were measured in the reactor core and at the flue gas. According to the results, the concentrations are very low at flue gases; nevertheless they are high at the reactor core. The HCN concentration is considerably higher than that of NH_3.

Godinho et al. (2006) presented an experimental analysis of a semi-pilot plant for the processing of footwear leather wastes. The objective of the work was to evaluate the performance of the plant. The unit comprises a stratified downdraft gasifier, an oxidation reactor and an air pollution control system (APC). The results obtained in this work led to conclude that the operational conditions applied in the process provided a low degree of oxidation of the chromium content in the waste. There is also a significant participation of water-soluble compounds in the particulate matter; the low concentration of CO in the flue gas indicates high combustion efficiency for the process. A significant reduction of the NO emissions was obtained, compared to the results of the combustion of footwear leather waste in fluidized bed. The main conclusion is that the footwear leather waste (biomass) represents an alternate source for the generation of energy. In another work, Shin et al. (2008) presents an investigation about the combustion characteristics of gas fuel in a pyrolysis-melting incinerator. The study aims to develop a novel incineration process considering the intrinsic characteristics of waste generated in Korea. The effects of secondary and tertiary air on flow pattern, mixing, and NO_x emissions of the combustion chamber were investigated. The pyrolyzed gas was simulated by propane, a mid-sized molecule among all the components. The propane was injected in the combustion chamber, and burnt through multi-step combustion by distributing the combustion air to primary, secondary, and tertiary air nozzles. Temperature and gas components in the combustion performances were determined by temperature distribution and O_2, CO and NO_x chemical species concentration. These results conclude that using the secondary and/or tertiary air, the combustion performance was improved, and, in particular, NO_x concentration decreased significantly following the tertiary air injection.

Salvador et al. (2006) presented a numerical 2D model to simulate the coupled equations for flow, heat transfer, mass transfer and progress of chemical reactions of a thermal recuperative incinerator (TRI) used to oxidize volatile organic compounds (VOCs) diluted in an air flow. The commercial software Fluent (Fluent Inc., 1998) was used. This model was confronted with experimental values obtained on a highly instrumented semi-industrial-scale pilot unit running under the same conditions. The results show that the model developed is a good tool for the analysis of combustion processes and it can predict important information about the flow, heat transfer and pollutant formation.

The work of Choi and Yi (2000) presented a numerical study of a combustion process of VOCs in a regenerative thermal oxidizer (RTO). Steady and unsteady flow field, distributions of temperature, pressure and compositions of the flue gas in the RTO were simulated by computational fluid dynamics (CFD) using the commercial software Fluent (Fluent Inc., 1998). The model system was the oxidation of benzene, toluene and xylene by the RTO, which was constituted by three beds packed with ceramic beads to exchange heat. The results show that a level of 1.0% of VOCs is sufficient to provide energy for the oxidation when heat is exchanged through the ceramic bed. A ceramic bed of 0.2 m in height is sufficient to operate properly at these conditions and 5 s is recommended as the stream switching time. In addition, the results can provide insight and practical responses involved in the design of an industrial RTO unit.

The objective of this work was the numerical study of the influence of moisture in the fuel gas on the combustion process of gases produced by the gasification of leather residuals, in furnaces of steam generators, in searching for data for the burning process optimization and the elimination of pollutants. Commercial software of CFD, CFX © Ansys Europe Ltd. was used. Through this study it was possible to investigate the influence of the moisture content on burning efficiency, temperature fields, heat transfer and specially, pollutant generation.

2. MATHEMATICAL FORMULATION

The proposed task can be stated as follows: design a combustion chamber to burn leather residual gasification gas in air, compute the temperature, chemical species concentrations and the velocity fields for gas mixture, and verify geometry features on the combustion process and pollutant formation.

The chemical reaction of the leather residual gasification gas used at this work, that here is considered composed to methane, hydrogen, carbon monoxide, is modeled according to global equations presented on Westbrook and Dryer (1981), which follow:

The methane oxidation is modeled by two global steps, given by:

$$2CH_4^{(16)} + 0{,}22N_2^{(28)} + 3(O_2^{(32)} + 3{,}76N_2^{(28)}) \rightarrow 2CO^{(28)} + 4H_2O^{(18)} + 11{,}5N_2^{(28)} \quad (1)$$
$$2CO^{(28)} + 1(O_2^{(32)} + 3{,}76N_2^{(28)}) \rightarrow 2CO_2^{(44)} + 3{,}76N_2^{(28)}$$

The toluene oxidation is modeled by two global steps, given by:

$$2C_7H_8^{(92)} + 11(O_2^{(32)} + 3{,}76N_2^{(28)}) \rightarrow 14\,CO^{(28)} + 8H_2O^{(18)} \quad (2)$$
$$2CO^{(28)} + (O_2^{(32)} + 3{,}76N_2^{(28)}) \rightarrow 2CO_2^{(44)} + 3{,}76N_2^{(28)}$$

The carbon monoxide oxidation is modeled by:

$$2CO^{(28)} + 1(O_2^{(32)} + 3{,}76N_2^{(28)}) \rightarrow 2CO_2^{(44)} + 3{,}76N_2^{(28)} \quad (3)$$

The hydrogen oxidation is modeled by:

$$2H_2^{(2)} + O_2^{(32)} \rightarrow 4H_2O^{(18)} \tag{4}$$

The formation of NO_x is modeled by Zeldovich mechanisms using two different paths, the thermal-NO and the prompt-NO, where the first, that is predominant at temperatures above 1800 K, is given by tree-step chemical reaction mechanisms:

$$O^{(16)} + N_2^{(28)} \rightarrow 2NO^{(30)} + N^{(14)} \tag{5}$$
$$N^{(14)} + O_2^{(32)} \rightarrow NO^{(30)} + O^{(16)} \tag{6}$$

In sub or near stoichiometric conditions, a third reaction is also used

$$OH^{(17)} + N^{(14)} \rightarrow NO^{(30)} + H^{(1)} \tag{7}$$

where the chemical reaction rates are predicted by Arrhenius equation.

The prompt-NO is formed at temperatures lower than 1800 K, where radicals can react rapidly with molecular nitrogen to form HCN, which may be oxidized to NO under flame conditions. The complete mechanism is not straightforward. However, De Soete proposed a single reaction rate to describe the NO source by Fennimore mechanism, which is used at this work. Arrhenius equations are used for predict this chemical reaction rate. At this way, the HCN oxidation to form NO is modeled by:

$$HCN^{(27)} + O_2^{(32)} \rightarrow HCO^{(29)} + NO^{(30)} \tag{8}$$

The HCN oxidation to consume the NO is

$$HCN^{(27)} + NO^{(30)} \rightarrow HCO^{(29)} + N_2^{(28)} \tag{9}$$

The HCO oxidation is modeled by

$$HCO^{(29)} + 0{,}75O_2^{(32)} \rightarrow CO_2^{(44)} + H_2O^{(18)} \tag{10}$$

And, to the reburn of NO by the CH_4 fuel gas

$$CH_4^{(16)} + 4NO^{(30)} \rightarrow CO_2^{(44)} + 4H_2O^{(16)} + 2N_2^{(28)} \tag{11}$$

Scalar transport equations are solved for velocity, pressure, temperature and chemical species.

2.1. Mass and species conservation

Each component has its own Reynolds-averaged equation for mass conservation, which, considering incompressible and stationary flow can be written in tensor notation as a mixture faction of all components. So, the standard continuity equation can be written as

$$\frac{\partial(\tilde{\rho}_i \tilde{U}_j)}{\partial x_j} = 0 \tag{12}$$

where $\tilde{U}_j = \sum \partial(\tilde{\rho}_i \tilde{U}_{ij})/\bar{\rho}$, $\tilde{\rho}_i$ and $\bar{\rho}$ are respectively the mass-average density of fluid component i in the mixture and the average density, x is the spatial coordinate, and $\tilde{U}_{ij}$ is the mass-averaged velocity of fluid component i.

The mass fraction of component i is defined as $\tilde{Y}_i = \tilde{\rho}_i/\bar{\rho}$. Substituting this expressions into Eq. (12) and modeling the turbulent scalar flows using the eddy dissipation assumption it follows that

$$\frac{\partial}{\partial x_j}\left(\bar{\rho}\,\tilde{U}_j\,\tilde{Y}_i\right) = \frac{\partial}{\partial x_j}\left(\left(\rho D_i + \frac{\mu_t}{Sc_t}\right)\frac{\partial \tilde{Y}_i}{\partial x_j}\right) + S_i \tag{13}$$

where D_i is the kinematic diffusivity, μ_t is the turbulent viscosity and Sc_t is the turbulent Schmidt number. Note that the sum of component mass fractions over all components is equal to one.

2.2. Momentum conservation

For the fluid flow the momentum conservation equations are given by:

$$\frac{\partial}{\partial x_j}\left(\bar{\rho}\,\tilde{U}_i\,\tilde{U}_j\right) = -\frac{\partial p^*}{\partial x_j}\delta + \frac{\partial}{\partial x_j}\left(\mu_{eff}\,\frac{\partial \breve{U}_i}{\partial x_j}\right) + \frac{\partial \tilde{U}}{\partial x_i \partial x_j} + S_u \tag{14}$$

where $\mu_{eff} = \mu + \mu_t$ and μ is the mixture dynamic viscosity and μ_t is the turbulent viscosity, defined as $\mu_t = C_\mu \rho k^2/\varepsilon$. The term $p^* = \bar{p} - (2/3)k$ is the modified pressure, C_μ is an empirical constant of the turbulence model, $\bar{p}$ is the time-averaged pressure of the gaseous mixture, and δ is the Krönecker delta function. S_u is the source term, introduced to model the buoyancy and drag force due to the transportation particles, and other mathematical terms due to turbulence models. The Boussinesq model is used to represent the buoyancy force due to density variations.

2.3. The $k - \varpi$ turbulence model

The equations for turbulent kinetic energy, *k*, and its turbulent frequency, ϖ, are:

$$\frac{\partial}{\partial x_j}\left(\tilde{\rho}\,\tilde{U}_j\,k\right) = \left(\frac{\partial}{\partial x_j}\left(\mu + \frac{\mu_t}{\sigma_k}\right)\frac{\partial k}{\partial x_j}\right) + P_k - \beta'\rho k\varpi \tag{15}$$

$$\frac{\partial}{\partial x_j}\left(\tilde{\rho}\,\tilde{U}_j\,\varpi\right) = \left(\frac{\partial}{\partial x_j}\left(\mu + \frac{\mu_t}{\sigma_\varpi}\right)\frac{\partial \varpi}{\partial x_j}\right) + \alpha\frac{\varpi}{k}P_k - \beta\rho\varpi^2 \tag{16}$$

where β', β, and α are empirical constants of the turbulence model, σ_k and σ_ϖ are the Prandtl numbers of the kinetic energy and frequency, respectively, and P_k is the term who accounts for the production or destruction of the turbulent kinetic energy.

$$P_k = \mu_t\left(\frac{\partial U_i}{\partial x_j} + \frac{\partial U_j}{\partial x_i}\right) \tag{17}$$

2.4. Energy conservation

Considering the transport of energy due to the diffusion of each chemical species, the energy equation can be written as

$$\frac{\partial}{\partial x_j}\left(\bar{\rho}\,\tilde{U}_j\,\tilde{h}\right) = \frac{\partial}{\partial x_j}\left(\left(\frac{k}{c_p}\right)\frac{\partial \tilde{h}}{\partial x_j} + \sum_i^{Nc}\bar{\rho}D_i\tilde{h}_i\frac{\partial \tilde{Y}_i}{\partial x_j} + \frac{\partial \mu_t}{Pr_t}\frac{\partial \tilde{h}}{\partial x_j}\right) + S_{rad} + S_{rea} \tag{18}$$

where $\tilde{h}$ and c_p are the average enthalpy and specific heat of the mixture. The latter is given by $c_p = \sum_\alpha \tilde{Y}_\alpha c_{p,\alpha}$, where $c_{p,\alpha}$ and $\tilde{Y}_\alpha$ are the specific heat and the average mass fraction of the α-th chemical species, k is the thermal conductivity of the mixture, Pr_t is the turbulent Prandtl number, and S_{rad} and S_{rea} represent the sources of thermal energy due to the radiative transfer and to the chemical reactions. The term S_{rea} can be written as:

$$S_{rea} = \sum_\alpha\left[\frac{h_\alpha^0}{\overline{MM}_\alpha} + \int_{\tilde{T}_{ref,\alpha}}^{\tilde{T}} c_{p,\alpha}d\tilde{T}\right]\overline{R_\alpha} \tag{19}$$

where $\tilde{T}$ is the average temperature of the mixture, h_α^0 and $\tilde{T}_{ref,\alpha}$ are the formation enthalpy and the reference temperature of the α-th chemical species. To complete the model, the density of mixture can be obtained from the ideal gas equation of state (Kuo, 1996; CFX Inc., 2004; Turns, 2000), $\bar{\rho} = p\overline{MM}\,(\bar{R}\tilde{T})^{-1}$, where p is the combustion chamber operational pressure, which is here set equal to 1 atm (Spalding, 1979), and $\overline{MM}$ is the mixture molecular mass. The aforementioned equations are valid only in the turbulent core, where $\mu_t \gg \mu$. Close to the wall, the logarithmic law of the wall is used (Launder and Sharma, 1974).

To consider thermal radiation exchanges inside the combustion chamber, the Discrete Transfer Radiation Model - DTRM is employed (Carvalho *et al.*, 1991), considering that the scattering is isotropic. The effect of the wavelength dependence is not considered, and the gas absorption coefficient is considered uniform inside the combustion chamber and its value is 0.5 m^{-1}. Then, the Radiative Transfer Equation – RTE is integrated within its spectral band and a modified RTE can be written as

$$\frac{dI(r,s)}{dS} = \frac{K_a\sigma\tilde{T}^4}{\pi} - K_a I(r,s) + S'' \tag{20}$$

At the equations above, σ is the Stefan-Boltzmann constant (5.672 x 10^{-8} W/m^2K^4), r is the vector position, s is the vector direction, S is the path length, K_a is the absorption coefficient, I is the total radiation intensity which depends on position and direction, and S'' is the radiation source term, which can incorporate the radiation emission of the particles, for example.

2.5. The E-A (Eddy Breakup – Arrhenius) chemical reactions model

The reduced chemical reactions model that is employed here assumes finite rate reactions and a steady state turbulent process to volatiles combustion. In addition, it is considered that the combined pre-mixed and non-premixed oxidation occurs in two global chemical reaction steps, and involves the follow species: oxygen, methane, hydrogen, nitrogen, water vapor, carbon dioxide and carbon monoxide. A conservation equation is required for each species, with the exception of nitrogen. Thus, one has the conservation equation for the α-th chemical species, given by Eq. (13), where the source term, S_i, considers the average volumetric rate of formation or destruction of the α-th chemical species at all chemical reactions. This term is computed from the summation of the volumetric rates of formation or destruction in all the *k*-th equations where the α-th species is present, $\overline{R_{\alpha,k}}$. Thus, $\overline{R_\alpha} = \sum_k \overline{R_{\alpha,k}}$.

The rate of formation or destruction, $\overline{R_{\alpha,k}}$, can be obtained from an Arrhenius kinetic rate relation, which takes into account the turbulence effect, such as Magnussen equations (Eddy Breakup) (Magnussen and Hjertager, 1976), or a combination of the two formulations, the so called Arrhenius-Magnussen model (Eaton *et al.*, 1999; CFX Inc., 2004). Such relations are appropriate for a wide range of applications, for instance, laminar or turbulent chemical reactions with or without pre-mixing. The Arrhenius equation can be written as follows:

$$\overline{R_{\alpha,k,Chemical}} = -\eta_{\alpha,k}\overline{MM}_\alpha \tilde{T}^{\beta_k} A_k \Pi_\alpha \tilde{C}_\alpha^{\gamma_{\alpha,k}} \exp\left(-\frac{E_k}{\bar{R}\tilde{T}}\right) \tag{21}$$

where β_k is the temperature exponent in each chemical reaction *k*, which is obtained empirically together with the energy activation E_k and the coefficient A_k. Π_α is the product symbol, $\tilde{C}_\alpha$is the molar concentration of the α-th chemical species, $\gamma_{\alpha,k}$ is the concentration exponent in each reaction *k*, $\bar{R}$ is the gas constant, $\overline{MM}_\alpha$ and $\eta_{\alpha,k}$ are the molecular mass and the stoichiometric coefficient of α in the *k*-th chemical reaction.

In the Eddy-Breakup or Magnussen model, the chemical reaction rates are based on the theories of vortex dissipation in the presence of turbulence. Thus, for diffusive flames:

$$\overline{R_{\alpha,k,EBU}} = -\eta_{\alpha,k}\overline{MM}_\alpha A\bar{\rho}\frac{\varepsilon}{k}\frac{\tilde{Y}_{\alpha^*}}{\eta_{\alpha^*,k}\overline{MM}_{\alpha^*}} \tag{22}$$

where the index α^* represents the reactant α that has the least value of $\overline{R_{\alpha,k,EBU}}$.

In the presence of premixing, a third relation for the Eddy Breakup model is necessary, so that

$$\overline{R_{\alpha,k,Premixing}} = \eta_{\alpha,k}\overline{MM}_\alpha AB\bar{\rho}\frac{\varepsilon}{k}\frac{\sum_p \tilde{Y}_p}{\sum_p \eta_{p,k}\overline{MM}_p} \tag{23}$$

where the index *p* represents the gaseous products of the combustion. *A* and *B* are empirical constants that are set as 4 and 0.5 (Magnussen and Hjertager, 1976). Magnussen model, Eqs. (22) and (23), can be applied to both diffusive and pre-mixed flames, or for the situation where both flames coexist, taking the smallest rate of chemical reaction.

Finally, for the Arrhenius-Magnussen model, given by Eqs. (21), (22) and (23), the rate of formation or destruction of the chemical species is taken as the least one between the values obtained from each model. It follows that

$$\overline{R_{\alpha,k}} = \min\left(\overline{R_{\alpha,k,Chemical}}, \overline{R_{\alpha,k,EBU}}, \overline{R_{\alpha,k,Premixing}}\right) \tag{24}$$

3. COMBUSTOR DESCRIPTION

The combustor comprises four tubular segments. The segments are made of refractory concrete. The first two and the fourth segments have a coaxial external tube (jacket) that creates an annular region where air is preheated. The combustion chamber comprises the first segment of the combustor, where a mixture of primary air and fuel is injected. The secondary air is forced by a blower from the inlet at the upper region of the second segment through the annular tube and is injected into the combustion chamber by means of several small holes evenly distributed along the first segment. The auxiliary air that enters at the lower part of the fourth segment is preheated at the annular region, then premixed with fuel oil and injected through the two auxiliary burners (Fig. 1) during the startup of the plant. After the startup period, the auxiliary burners act as tertiary air feeders.

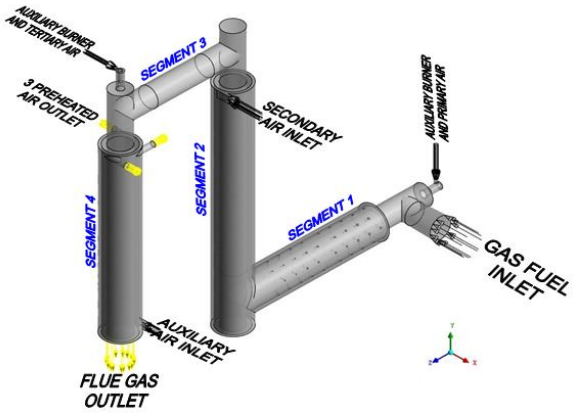

Figure 1. General disposition of the combustor.

4. MESH SETTINGS AND CONVERGENCE CRITERIA

The domain under consideration comprises the combustor of a gasification/combustion plant to convert biomass in energy: the combustor comprises a tubular riser where occurs the combustion process of residual gasification gas as showed at Fig. 1. The entrance to combustor was considered the outlet of the domain. The discretization was done using tetrahedral volumes. Prismatic volumes were used at the walls in order to capture the boundary layer behavior and mesh refinements in the entrance region, corresponding to the first part of the combustor. Due to computational limitations, the mesh size used has approximately 2.8 $x10^6$ elements. The convergence criterion adopted was the RMS – Root Mean Square of the residual values, and the value adopted was $1x10^{-6}$ for all equations.

5. BOUNDARY CONDITIONS

The gas of leather residuals gasification process was modeled in this study as a fuel with C_7H_8, H_2O, N_2, CO, H_2, HCN and CH_4, as shown in Tab. 1. The mass fraction (kg/kg_{fuel}), fraction (%) and mass flow (kg/h) of each component are also presented in the table. The gas inlet mass flow considered was 800 kg/h, with a uniform temperature of 800 ^oC. This value for the temperature was selected considering the former gasification process, not presented in this work.

Table 1: Chemical composition of the inlet gas.

Components	Mass Fraction (kg/kg_{fuel})	Fraction (%)	Mass Flow (kg/h)
C7H8	0,001	0,10%	0,800
H2O	variable	variable	variable
O2	-	-	-
N2	variable	variable	variable
CO	0,032	3,20%	25,597
CO2	0,23	23,00%	183,982
H2	0,007	0,70%	5,599
CH4	0,012	1,20%	9,599
HCN	0,001	0,10%	0,800

In this work, some values (7.6%, 10%, 15% and 20% of humidity) of fuel moisture content were contrasted. The moisture content was set by reducing accordingly the Nitrogen content, in order to maintain the proportionality of the other gases. The role of the Nitrogen is secondary in the reaction, so this substitution is possible without lack of quality of the model. The air composition was set, as usual, by 23% of O_2 and 77% of N_2. The secondary air inlet temperature was the ambient temperature in the vicinity of the plant (25 ^oC) and the mass flow was taken to 720 kg/h. The auxiliary burners inlet air (primary and tertiary) is pre-heated at the segment four, with a mass flow set to 90 kg/h for each burner. The thermal conductivity of the reactor walls insulation is approximately 1.4 W/(m K) and the density is 2300 kg/m^3. The thermal conductivity of the walls was disregarded, as usual, due to the low influence in the calculations.

6. RESULTS

The results were obtained by applying the mass and momentum conservation equations for the fluid flows, considering the k-ω model to predict the turbulent behavior of the flows. The temperature dependence of the density

was considered for the gravity lift computation. The energy conservation equation is solved to predict the heat transfer rates an the temperature distribution field inside the combustion chamber. The chemical species conservation equations were solves along with the chemical reactions models, Eddy Breakup and Arrhenius (EBU-A). The thermal radiation model Discrete Transfer Radiation Model – DTRM was applied in order to allow the analysis of the influence of the radiation inside the chamber.

Figures 2-a and 2-b show the temperature field in the longitudinal plane during the burning of fuel with moisture content of 7,6% e 20% respectively. The temperature at the flame core is different at each Figure due to the moisture content: the higher the moisture content, the higher the quantity of energy used to evaporate all the water, and the lower will be the temperatures.

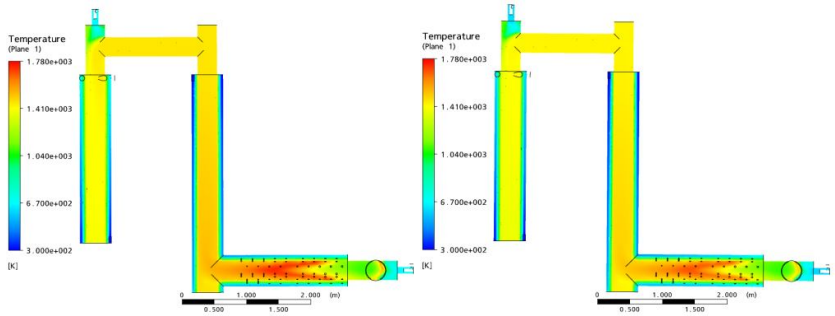

(a) (b)

Figure 2. (a) Temperature field (moisture 7.6%); (b) Temperature field (moisture 20%).

Figures 3-a and 3-b show the concentration of hydrogen and toluene in the same longitudinal plane. It was found that the mass fractions of hydrogen and toluene do not change in the combustion process with the variation of moisture in the fuel. The hydrogen is completely oxidized in the first half of the combustion chamber of the first segment. The same is true for toluene shown in Fig 3-b. This leads to the conclusion that the size of the combustion chamber is suitable for the operational parameters applied.

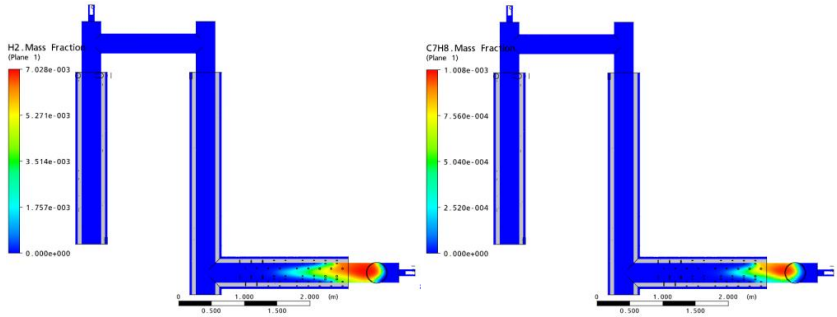

(a) (b)

Figure 3. (a) Concentration of hydrogen; (b) Concentration of Toluene.

Figures 4-a and 4-b show the results of concentration fields for CO and CH_4, which also do not that also do not vary with the fuel gas moisture content. The results of Figs. 3-a, 3-b, 4-a and 4-b indicate that all the fuel is oxidized in the first stage of the combustion chamber (segment 1) resulting in a flame that occupies the full length of it.

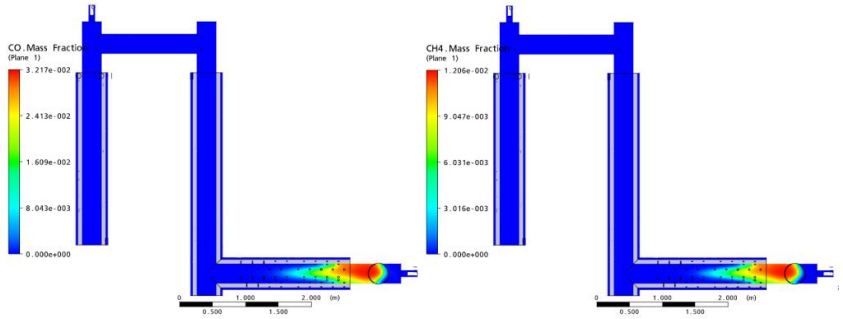

(a) (b)

Figure 4. (a) Concentration of carbon monoxide; (b) Concentration of methane.

Figure 5 shows the results of the oxygen concentration fields for moisture contents of 7.6% and 20%. In this figure it is observed that the highest concentration of oxygen is at the entrance of primary air and disappears progressively along the chamber because the oxygen is consumed by the combustion process. It is also observed that the mass fraction of oxygen increases slightly with increasing moisture in the fuel gas due to the increase of oxygen delivered by the molecules of H_2O

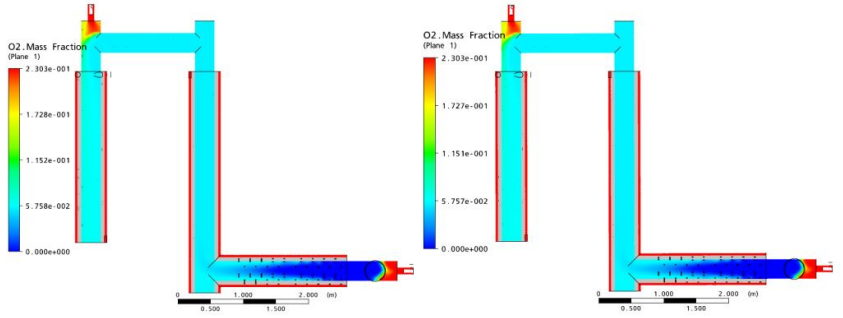

(a) (b)

Figure 5. (a) Oxygen concentration (7.6% moisture); (b) Concentration of oxygen (20% moisture).

Figure 6 shows the concentration of H_2O corresponding to moisture contents of 7.6% and 20% respectively.

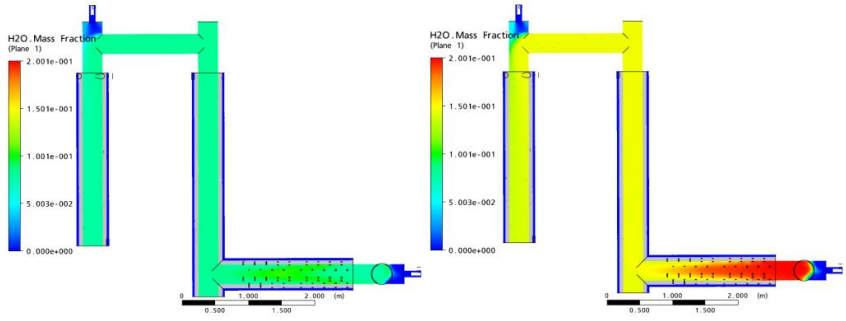

(a) (b)

Figure 6. (a) Concentration of water vapor (7.6% moisture); (b) concentration of water vapor (20% moisture).

Figure 7 shows the profiles of HCO concentrations along the reactor for different moisture levels. The simultaneous observation of Figure 2 (temperature fields) and Figure 7 (HCO concentration fields) allows verification that the production of HCO occurs in regions of higher temperatures in the combustion chamber which comprises the tip of the flame. The moisture content is responsible for the decrease of the temperature of the combustion process. One can observe that there is a slight increase (in order of ppm) of not oxidized HCO at the exit of the reactor (see Table 2). One can also observe that almost all HCO is oxidized along the combustion chamber.

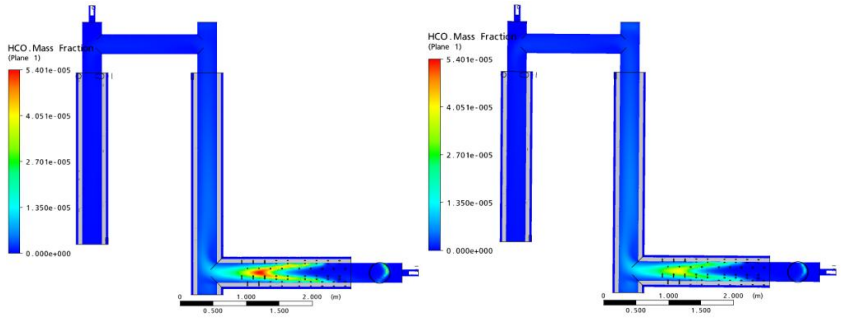

(a) (b)

Figure 7. (a) HCO concentration (7.6% moisture); (b) Concentration of HCO (20% moisture).

Figure 8 shows the concentration profiles of N_2 along the reactor, for different moisture levels. Nitrogen is considered an inert gas to the combustion process, participating in small quantities only in the formation of NO_x.

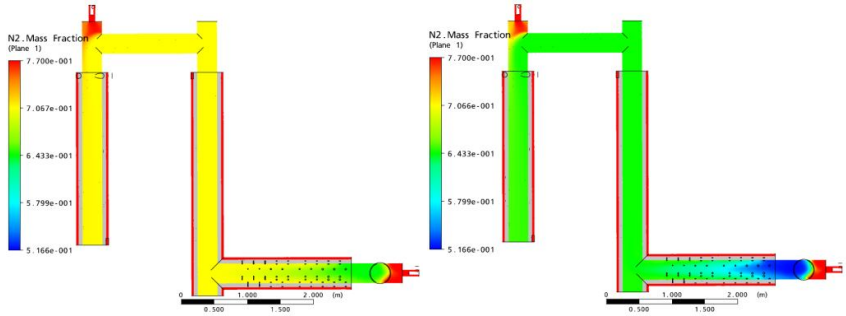

(a) (b)

Figure 8. (A) Nitrogen concentration (7.6% moisture); (b) Nitrogen concentration (20% moisture).

The HCN concentration fields for moisture contents of 7.6% and 20% are shown in Figure 9. The concentration of HCN is highest in the segment 1, the region with highest concentration of hydrogen (Fig. 3a) and also suffers slight increase in the output of the reactor with increasing humidity. In the next segment the combustion products are diluted with the secondary and tertiary air.

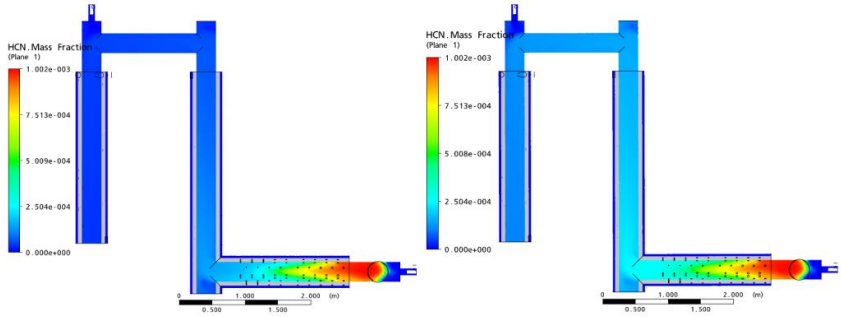

(a) (b)

Figure 9. (A) Concentration of HCN (7.6% moisture); (b) Concentration of HCN (20% moisture).

The concentration fields of NO_x (Thermal + Prompt + Fuel) for different moisture contents in the fuel are shown in Figure 10.

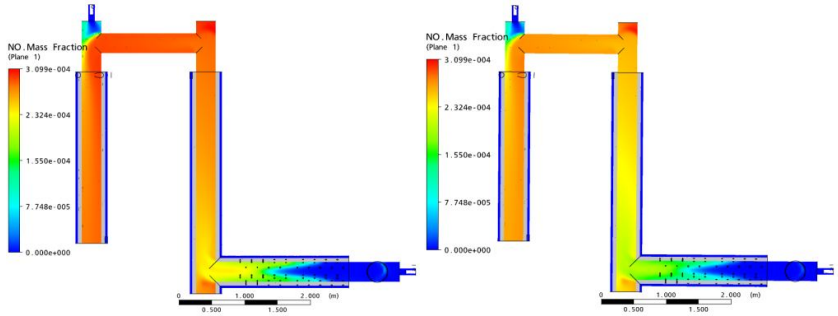

(a) (b)

Figure 10. (A) NO_x concentration (7.6% moisture); (b) NO_x concentration (20% moisture).

Figure 10 also shows that there is a high rate of NO_x formation along the reactor, especially in the combustion chamber, where temperature is higher. Figure 2 shows the temperatures around 1300-1500 K, high enough to increase the production of NO_x by the mechanism of Fennimore. It can be seen then that the increase of moisture in the fuel decreases the production of NO_x by lowering the temperature inside the combustion chamber, which is desirable. Comparing the fields of Figs. 9 and 10, one can observe that the concentrations of NO_x and HCN have an inverse relationship, the concentration of the last decreases as the concentration of the former increases. The higher level of excess air and the large residence time of combustion gases in the reactor also contribute, along with moisture, for the production of NO_x.

Table 2 presents the chemical composition of combustion gases (in ppm) in the output of the reactor, for different moisture contents, obtained with the simulations.

Table 2 - Concentration of the gases exiting the reactor for different moisture contents simulated.

	Outlet flue gas concentration for different humidities (ppm)			
Products	**7,60%**	**10%**	**15%**	**20%**
C7H8	0,00044	0,00044	0,00044	0,00044
CH4	0,0056	0,0056	0,0056	0,0056
CO	0,106	0,106	0,106	0,106
H2	0,0033	0,0033	0,0033	0,0033
CO2	149713,0	149698,0	149662,0	149607,0
H2O	78439,0	89730,70	113254,000	136773,0
O2	62195,90	62209,10	62244,30	62300,50
NO	283,089	283,229	279,670	268,526
N2	709330,0	698031,0	674490,0	650947,0
HCO	0,225	0,262	0,336	0,380
HCN	38,46	47,67	69,95	103,10

7. CONCLUSIONS

Analyzing the temperature fields obtained by the simulations for the two moisture contents presented (7.6% and 20% humidity), one can conclude that humidity has a significant importance in the process, because the higher the moisture content in the fuel the greater the energy used for evaporation of H_2O, consuming a larger amount of fuel to produce the same amount of useful energy. The variation of humidity has influence in the gases derived from combustion process, CO_2, O_2, NO, HCO and HCN, with a greater amount of O_2, HCN and HCO and a lower amount of CO_2 and NO with the increase of moisture content. The N_2 and H_2O concentrations in the fuel were set with an inverse relationship, one decreases while the other increases, this principle is used so that we can change the concentration of moisture in the fuel without changing the total mass flow entering the combustion chamber or the concentration of other gases present in the fuel. This is valid because the N_2 is an inert gas in the combustion process. The observation of the reduction of pollutants such as CO_2 and NO may induce thought that would be better to operate a Rankine cycle thermal plant with high moisture in the fuel, but this is not true. The higher the moisture content of fuel, the higher the portion of available heat that is expended to evaporate water, then leaving little thermal energy to heat the particles to the ignition temperature. All variables that affect the ignition also affect the combustion, such as moisture, which lowers the operating temperature of the plant, lowering also the plant efficiency. In addition, corrosion problems may appear due to the formation of acids from high concentration of water vapor in the flue gas.

8. ACKNOWLEDGEMENTS

The authors thank for the support of CNPq – National Research Council (Brazil) – by granting a research scholarship to the first author.

9. REFERENCES

Bahillo, A., Armesto, L., Cabanillas, A. and Otero, J., 2004. "Thermal valorization of footwear leather wastes in bubbling fluidized bed combustion". Waste Management, Vol. 24, pp. 935-944.

Carvalho, M.G., Farias, T. and Fontes, P., 1991. "Predicting radiative heat transfer in absorbing, emitting, and scattering media using the discrete transfer method", ASME HTD, Vol. 160, pp.17-26.

CFX Solver Theory, 2004.

Choi, B.S. and Yi, J., 2000. "Simulation and optimization on the regenerative thermal oxidation of volatile organic compounds". Chemical Engineering Journal, Vol. 73, pp. 103-114.

Eaton, A. M., Smoot, L. D., Hill, S. C. and Eatough, C. N., 1999, "Components, formulations, solutions, evaluations, and applications of comprehensive combustion models", V. 25, pp. 387-436.

Fluent User's Guide, vol. 2, 1998.

Godinho, M., 2006 "Gaseificação e combustão de resíduos sólidos da indústria calçadista". Doctoral Thesis, Programa de Pós-Graduação em Engenharia de Minas, Metalúrgica e de Materiais (PPGEM), Universidade Federal do Rio Grande do Sul, Brazil.

Godinho, M., Marcilio, N.R., Faria Vilela, A.C., Masotti, L. and Martins, C.B. 2007 "Gaseification and combustion of the footwear leather wastes". Jalca, Vol. 102, pp. 182-190

Kuo, K.K., 1996. "Principles of combustion", John Wiley & Sons, New York.

Launder, B.E. and Sharma, B.I., 1974. "Application of the energy-dissipation model of turbulence to the calculation of flow near a spinning disc", Letters in Heat and Mass Transfer, Vol. 19, pp. 519-524.

Magnussen B.F. and Hjertager B. H., 1976. "On mathematical models of turbulent combustion with special emphasis on soot formation and combustion". Proc. of the 16th Int. Symp. on Comb., The Combustion Institute, pp. 719–729.

Salvador, S., Commander, J.M. and Kara, Y., 2006. "Thermal recuperative incineration of VOCs: CFD modeling and experimental validation". Applied Thermal engineering, Vol. 26, pp. 2355-2366.

Shin, D., Yu, T., Yang, W., Jeon, B., Park, S. and Hwang, J., 2008. "Combustion characteristic of simulated gas fuel in a 30 kg/h scale pyrolysis-melting incinerator". Waste Management, IN PRESS.

Spalding, D.B., 1979. "Combustion and Mass Transfer", Pergamon Press, Inc., New York.

Turns, S. T., 2000, "An introduction to combustion – Concepts and applications", 2nd ed, McGraw-Hill, New York.

Westbrook, C. K. and Dryer, F.L., 1981. "Simplified reaction mechanisms for the oxidation hydrocarbon fuels in flames". Comb. Sci. and Technology, Vol. 27, pp. 31-43.

RESPONSIBILITY NOTICE

The authors are the only responsible for the printed material included in this paper.